



Self-heating evaluation on thermal analysis of polymethyl methacrylate (PMMA) and linear low-density polyethylene (LLDPE)

Alain Alonso¹ · David Lázaro¹ · Mariano Lázaro¹ · Daniel Alvear²

Received: 30 November 2021 / Accepted: 4 April 2022 / Published online: 29 April 2022
© The Author(s) 2022

Abstract

Thermal analysis has been proven to be an efficiently technique to analyse thermal decomposition reactions of different type of materials. This technique is widely used in different fields. Among them, fire science, where polymeric materials are very common, has a particular issue, being the combustion reactions recurrent on these analyses. Thermal analysis has different particularities depending on the studied material. For instance, polymeric materials could undergo different decomposition reactions that are highly dependent on definition of the thermal analysis boundary conditions. The International Confederation for Thermal Analysis and Calorimetry (ICTAC) (Vyazovkin et al. in *Thermochim Acta* 590:1–23, 2014) and standards (ISO 11358-1. Plastics—Thermogravimetry (TG) of polymers—Part 1: General principles. ISO. 2014; <https://www.iso.org/standard/59710.html>. Accessed 31 Jan 2022), (ISO 11357-1. Plastics — Differential scanning calorimetry (DSC) — Part 1: General principles. ISO. 2016; <https://www.iso.org/standard/70024.html>. Accessed 31 Jan 2022) establish how to set-up these boundary conditions in the thermogravimetric (TG) and differential scanning calorimetry (DSC) standards. As far as initial amount of sample mass is concern, some discrepancies can be found between the standards. For instance, the standards suggest a sample mass between 10 and 100 mg for TG and between 2 and 40 mg for DSC, whereas the ICTAC recommendations suggests that the sample mass times the heating rate should not exceed $100 \text{ mg K}\cdot\text{min}^{-1}$ in thermo-oxidative decomposition analysis, which is equivalent to samples masses lower than 10 mg for heating rates of $10 \text{ K}\cdot\text{min}^{-1}$, or lower than 5 mg for heating rates of $20 \text{ K}\cdot\text{min}^{-1}$. This discrepancy may lead to obtain different results from the tests. Additionally, according to the thermal and thermo-oxidative decomposition of polymers, the ICTAC remarks the influence on the results of the sample thicknesses, carrier gas and heating rates, but it does not analyse the influence of self-heating as it does for the hazardous materials. This work presents a study of the self-heating influence in the thermal decomposition processes of two widely used polymers as poly methyl methacrylate (PMMA) and linear low-density polyethylene (LLDPE). TG/DSC tests are used to evaluate the thermal decomposition processes. Boundary conditions of the tests definition as sample mass, atmospheres, and heating rate are considered to evaluate its influence on the polymers self-heating effect on the thermal decomposition. It also includes how to check if TG/DSC tests follows the theoretical principles of the thermal analysis, or if the results are affected by the self-heating. In the present study, a series of 32 experimental tests has been performed, analysing 16 boundary conditions. These experimental tests allow evaluating the influence of selected boundary conditions on the mass loss, the heat flux, and the materials decomposition reactions. Additionally, we analyse the effect of the boundary conditions on the temperature of the sample. Results show the impact of each different boundary conditions of the self-heating effect, and its influence in the final thermal decomposition measured and they represent an aid to define the suitable conditions to perform TG/DSC test on PMMA and LLDPE, or similar polymer materials. This is done by the evaluation of the influence of the self-heating in parameters as the sample temperature lags defined in [1], the reactions heat fluxes, and the difference between the sample and the programmed temperature. It is also analysed the influence of the auto-ignition temperature in the thermal analysis. It is remarkable the PMMA auto-ignition temperature effect on the TG/DSC results. Finally, some useful recommendations have been defined.

Keywords Thermal analysis · Polymeric materials · DSC · TGA

List of symbols

Abbreviations

Al ₂ O ₃	Alumina
MLR	Mass loss rate
ASTM	American Society for Testing and Materials
LLDPE	Linear low-density polyethylene
DTG	Derivative Thermogravimetry
PMMA	Poly methyl methacrylate
DSC	Differential Scanning Calorimetry
pDSC	Peak DSC
ICTAC	International Confederation for Thermal Analysis and Calorimetry
PVC	Polyvinyl chloride
ISO	International Organization for Standardization
STA	Simultaneous Thermal Analysis

Letters

C_p	Specific heat/ $\text{kJ}\cdot\text{kg}^{-1}\cdot\text{K}^{-1}$
T_{fur}	Furnace temperature/ $^{\circ}\text{C}$
m	Mass/mg
T_{sam}	Sample temperature/ $^{\circ}\text{C}$
O ₂	Oxygen concentration/%
T_{pro}	Programmed temperature/ $^{\circ}\text{C}$
N ₂	Nitrogen concentration/%
ΔH_{chem}	Chemical heat of combustion/ $\text{kJ}\cdot\text{g}^{-1}$

Greek letters

α	Diffusivity/ $\text{mm}^2\cdot\text{s}^{-1}$
ρ	Density/ $\text{kg}\cdot\text{m}^{-3}$
k	Thermal conductivity/ $\text{W}\cdot\text{m}^{-1}\cdot\text{K}^{-1}$

Introduction

Thermogravimetric analysis (TG) is a useful experimental technique to analyse the behaviour of a material when increases its temperature due to an external heat source, in other words, how the mass is loss with the temperature obtaining the TG curve or its derivative DTG (Derivative Thermogravimetry) curve. Thermogravimetric tests are carried out inside a fully controlled atmosphere, e.g., inside a small-enclosed furnace and the mass of the tested samples has an order of magnitude of milligrams. TG tests can be performance simultaneously with DSC test (Differential Scanning Calorimetry) that measure the energy released by the sample during the heating process, obtaining the DSC curve. When both tests are carried out simultaneously, they are known as STA (Simultaneous Thermal Analysis).

On the one hand, the fully control of the TG apparatus allows defining several boundary test conditions such as: heating program (isothermal, non-isothermal or quasistatic); the atmosphere of the furnace (air, nitrogen, argon, corrosive atmosphere, vacuum, etcetera); the material of the crucible

(alumina, gold, platinum); the employment of a lid for the crucible; the state of the sample (solid, powder, chopped, etcetera) or the initial amount of mass sample. On the other hand, either the high precision of the analysis results or the influence of the boundary conditions could alter the results.

Obtaining a reliable STA curves represents a key factor in fire engineering. These curves are employed to characterize the kinetic of the material, habitually using the Arrhenius equation [4] and several techniques such as numerical methods [5, 6] (model fitting, model-free) or optimization methods (inverse modelling) [7–9].

Therefore, it seems to be important knowing which the best boundary conditions are to carry out a thermogravimetric test. Some of these boundary conditions can be determined taking into account other studies in similar conditions from available literature. For instance, in fire engineering non-isothermal heating rates are employed to carry out STA and DSC tests [10–12]; the material of the crucible should be chosen in order to avoid the reaction with the sample [13]; or the condition of the sample which is recommended to be in powder for solids as far as possible [1].

However, not all boundary conditions are well defined. In this way, some contradictions can be found concerning the heating rate and the initial amount of mass of the sample.

As far as the heating rate is concern, despite the recommended heating (and cooling) rates should have few degrees only [1], works available in the literature using a wide range of heating rate. Among others: in [14] authors employ up to a heating rate of $100\text{ K}\cdot\text{min}^{-1}$ to identify the kinetics of biomass decomposition in oxidative atmospheres; the authors of [15] use a heating rate up to $50\text{ K}\cdot\text{min}^{-1}$ in oxidative atmosphere to analyse combustion of corncob and stover; or in [16] the authors used three heating rates (5, 10 and $20\text{ K}\cdot\text{min}^{-1}$) in oxidative and non-oxidative atmosphere to elaborate two kinetic models (one for atmosphere) to predict the thermal behaviour of three materials. Related with the heating rate, the reactive chemical effect also play a factor that should have into account. The reactive nature of some materials, either exothermic or endothermic decomposition processes, could produce that surrounding temperatures of the sample increase or decrease. In order to reduce this effect, it is recommended using slow heating rates for these tests [1]. This effect has been analysed in several works such as [17–20].

As to initial mass of the sample, the standards [2, 3] and the International Confederation for Thermal Analysis and Calorimetry (ICTAC) recommendations [1] indicate, among other features, the amount of mass should be take into account for carry out a thermogravimetric test (TG) and differential scanning calorimetry test (DSC). Some differences related with this initial amount of mass can be found. Whereas, the standards suggest sample masses between 10 and 100 mg for TG [2] and between 2 and

40 mg for DSC [3], the ICTAC recommendations [1] suggest that the sample mass times the heating rate should not exceed $100 \text{ mg K}\cdot\text{min}^{-1}$ to thermo-oxidative decomposition analysis, which is equivalent to samples masses lower than 10 mg for heating rates of $10 \text{ K}\cdot\text{min}^{-1}$, or smaller than 5 mg for heating rates of $20 \text{ K}\cdot\text{min}^{-1}$. That discrepancy may lead to obtain different results from the tests. For instance, several works have evaluated the influence of the sample mass, through experimental tests, in the thermal decomposition reactions [17, 18]. Additionally, according to the thermal and thermo-oxidative decomposition of polymers, the ICTAC remarks the influence on the results of the sample thicknesses, carrier gas and heating rates, but it does not analyse the influence of self-heating as it does for the hazardous materials.

The influence of the STA boundary conditions in the thermal decomposition of thermoplastic polymers is analysed in [21]. This study analysed the influence of the initial sample mass, the carrier gas, the heating rates, the sample holder and the gas flow on the thermal decomposition. This work concluded, in line with [1], that initial sample mass and heating rate might affect the obtained TG/DSC curves. Furthermore, it is shown that some materials such as LLDPE, could produce a considerable amount of energy in certain conditions during its decomposition. Nevertheless, it is not defined how to check if certain experimental tests results are affected or not by the energy release during the decomposition reactions.

Some results collected in the literature [22, 23] seem to reflect the self-heating effect on the decomposition process results of different non-hazardous materials. In [22], where the authors studied pyrolysis and combustion characteristics of some types of pellets, the TG and DTG curves of some test under air atmosphere show an unusual behaviour, similar to the effect shown in [1] and associated with the self-heating phenomenon. This phenomenon is reflected in the TG curves with the appearance of several values of the sample mass (or equivalent extent of conversion) for a single value of temperature. These unusual results are not explained in [22]. The same deviation of the TG is shown in [23], where the authors analyse corn stover. In this work, authors suggest that this effect is associated with the high exothermic process that leads to a great increase of the temperature that the control system of the thermobalance attempts to compensate. Nevertheless, they do not analyse in deep where these singularities come from.

Taking into account these aspects, this work aims to analyse how the potential appearance of the self-heating event during the execution of a STA test may affect the TG and DSC curves for polymeric materials. Moreover, this work analyses under which boundary conditions self-heating effect could take place, focus on the influence of three boundary conditions: initial sample mass, heating rate

and oxygen level. Finally, the influence of the auto-ignition temperature [24] of the analysed materials is also analysed. To deal with the objective, this work monitors the temperatures of the test, in particular, the furnace temperature (T_{fur}) and sample temperature (T_{sam}) and relates their behaviour with the mass loss rate (TG) and energy released (DSC) curves. In light of the results, on the one hand, under oxidative atmosphere fast heating rates and moderate values of initial mass makes T_{sam} to have a non-constant rising slope affecting both TG and DSC curves. On the other hand under inert atmosphere, the T_{sam} tends to have a constant rising slope. Furthermore, the temperature lag (defined in next section) undergoes alterations when the T_{fur} and the T_{sam} have no constant growth.

Materials and method

In this work, we employed two polymers widely utilized: low-density polyethylene (LLDPE) and poly(methyl methacrylate) (PMMA). As these polymeric materials have a considerable amount chemical heat of combustion, this feature could lead to the appearance of a self-heating event during their thermal decomposition. The LLDPE is a polymer manufactured through the copolymerization of ethylene and α -olefins (comonomers) [25]. The thermal decomposition of the LLDPE is produced as a result of two main pathway: random chain scission and chain branching [26]. The chemical heat of combustion of the LLDPE is $38.4 \text{ kJ}\cdot\text{g}^{-1}$ [27] and the auto-ignition temperature is established around $350 \text{ }^\circ\text{C}$ [28].

The polymer poly(methyl methacrylate), PMMA, is a polymer made of a macromolecule (ethylene and one methyl group swapping one hydrogen atom), and a hydrogen atom which is replaced by an acetyl group [29]. The thermal decomposition process of the PMMA can be summarized as the combination of two main consecutive processes: main chain random scission and the homolytic scission of the methoxycarbonyl side group [30]. The value of the chemical heat of combustion of the PMMA is $24.2 \text{ kJ}\cdot\text{g}^{-1}$ [27], and its auto-ignition temperature is $380 \text{ }^\circ\text{C}$ [31, 32].

The analysis was conducted with the equipment Netzsch STA 449 F3. This apparatus allows testing samples within a range of temperatures between 30 and $1500 \text{ }^\circ\text{C}$ in several atmospheres, such as air or non-oxygen content (inert). The resolution for the temperature and mass measurements are 0.001 K and $0.1 \text{ }\mu\text{g}$ over the entire weighing range, respectively (up to $1500 \text{ }^\circ\text{C}$). The DSC enthalpy accuracy is $\pm 2\%$ for most materials. The employed crucibles are made of alumina (Al_2O_3) without lid.

In order to evaluate the appearance of the self-heating phenomenon and its influence on the thermal decomposition process, in this work, we executed up to 16 different tests varying the boundary conditions. Next Table 1 gathers the

Table 1 Boundary conditions: values of initial sample mass, oxygen concentration and heating rate

LLDPE				PMMA			
Test	Mass/mg	O ₂ /%	HR/K·min ⁻¹	Test	Mass/mg	O ₂ /%	HR/K·min ⁻¹
#1	11.849	20	10	#9	19.019	20	10
#2	1.288	20	10	#10	1.193	20	10
#3	26.878	0	10	#11	17.362	0	10
#4	12.514	20	20	#12	15.794	20	20
#5	1.110	20	20	#13	1.318	20	20
#6	11.763	20	50	#14	15.599	20	50
#7	1.198	20	50	#15	1.143	20	50
#8	11.584	0	50	#16	15.097	0	50

initial mass of the sample, the oxygen concentration and the heating rate for all boundary conditions tested. The utilised heating rates are 10, 20 and 50 K·min⁻¹. For each heating rate, with the exception of 20 K·min⁻¹, we analysed two types of atmospheres: air (20% O₂ and 80% N₂) and non-oxygen content (100% N₂). For oxygen-content atmospheres, we tested two types of initial amount of mass: low mass (less than 1,5 mg) recommended by the ICTAC [1], and high mass (between 10 and 30 mg) whose values are close to those recommended by the standards [2, 3]. Tests for non-oxygen content atmosphere have high initial mass uniquely.

To ensure the repeatability of the results, for every test condition, each polymer was tested two times. Once the repeatability was checked, in order to clarify the visibility of the curves in the graphics, it is only shown the results for one test for each boundary condition.

To cope with the objective of the work, the following outputs were monitored how the sample has been heated during the STA test: TG curve, DSC curve, T_{fur} , T_{sam} the programmed temperature (T_{pro}). The TG and DSC curves provides how the sample loss its mass and the energy released/absorbed as a function of the temperature of the sample as a function of time or T_{sam} . These both signals are the ones typically displayed as a result of a STA test. The mass is measured by the balance of the apparatus and the temperature difference between the sample and the empty crucible provides the energy released or absorbed in the DSC signal.

Additionally, we display the temperatures of three parts: T_{pro} , T_{fur} and T_{sam} . The T_{pro} corresponds to the one defined by the user in the heating program, calculated as the initial temperature plus the heating rate multiplied by the test elapsed time. T_{fur} measures the temperature of the furnace and the thermocouple to do it is located close to the measuring head that holds the crucibles (sample and reference). The T_{sam} represents the temperature of the sample. The thermocouple for measuring T_{sam} is located below the alumina crucible that contents the sample.

Once these three temperatures are measured, we built next two curves: the ($T_{\text{fur}} - T_{\text{sam}}$) and ($T_{\text{pro}} - T_{\text{sam}}$). They measure temperature differences between them during the heating

process, which are helpful to identify a self-heating event. The difference between ($T_{\text{fur}} - T_{\text{sam}}$) allows us to measure the temperature defined in [33], i.e., that represents that when the T_{fur} changes, the T_{sam} lags behind because it takes some time for heat from the furnace to transfer into the sample, determining the temperature lag between the furnace and the sample temperatures [1]. The curve ($T_{\text{pro}} - T_{\text{sam}}$) is expected to be close as possible to zero, i.e., the test apparatus tends to heat the sample following the pre-programmed temperature with small differences. We verified the deviation of this curve, as it is recommended in [1], especially for crystallization of inorganics and hazardous materials although the materials tested in this work are polymers.

Any fluctuation in the tendency of the ($T_{\text{fur}} - T_{\text{sam}}$) curve and variation from zero values of the ($T_{\text{pro}} - T_{\text{sam}}$) curve could allow us to elucidate if a self-ignition event has been taken place during the test, how the TG and DSC have been altered due to it, and therefore, determine if the boundary conditions of the test are suitable.

Results

In order to identify the influence of the heating rate, sample mass initial mass and atmosphere in the performance of the thermogravimetric tests method, we organized, for each analysed material, the results as follows: firstly, TG and DSC curves; and secondly, the test temperatures measured. The tests temperatures curves are analysed comparing their differences ($T_{\text{fur}} - T_{\text{sam}}$) and ($T_{\text{pro}} - T_{\text{sam}}$) versus the T_{pro} . All curves are classified into three groups: (a) oxygen content atmosphere high mass, (b) oxygen content atmosphere low mass, (c) non-oxygen content atmosphere.

LLDPE

Figure 1 compares the LLDPE TG and DSC curves as a function of the T_{sam} . The vertical dash dot line indicates the auto-ignition temperature of the LLDPE, 350 °C.

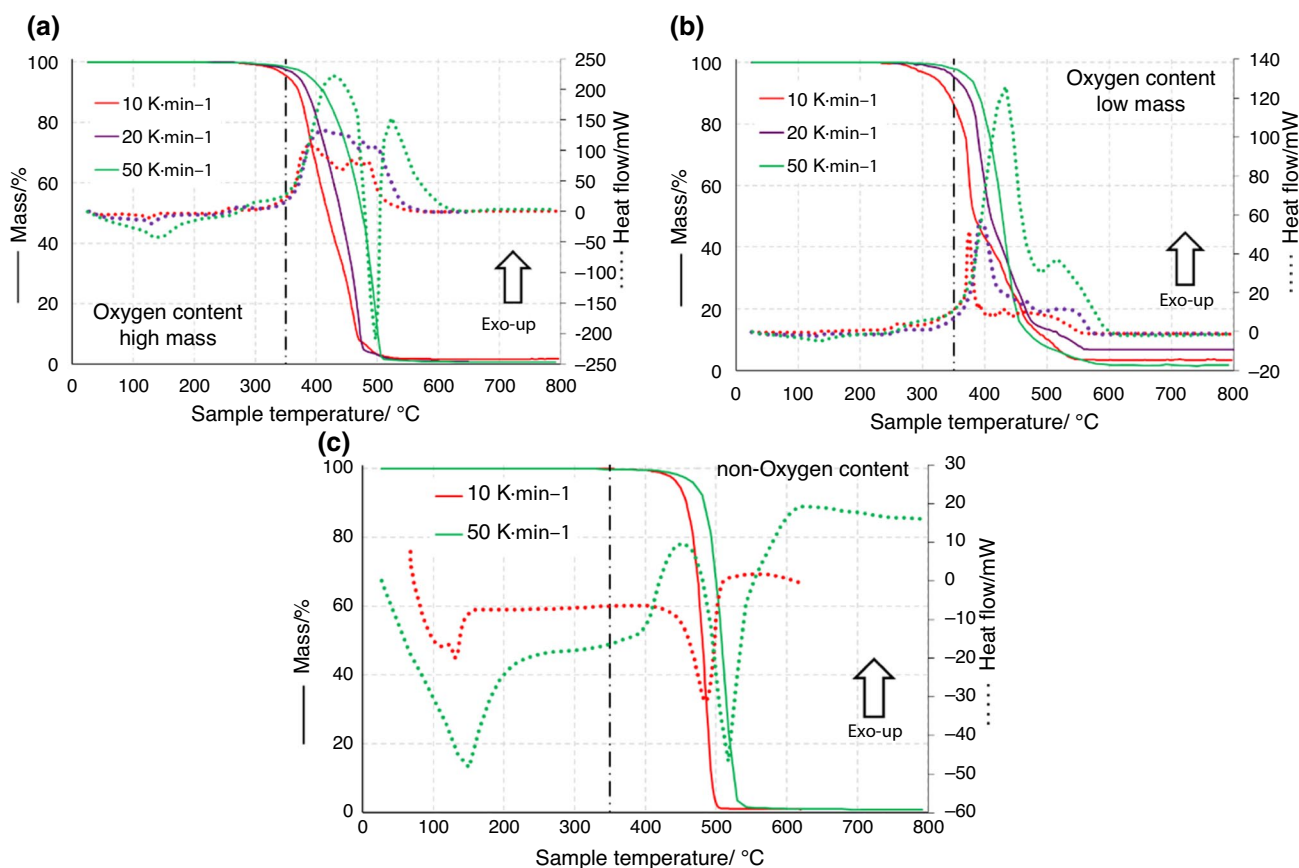


Fig. 1 LLDPE. Comparison TG and DSC curves at different heating rates: **a** oxygen-content and high mass; **b** oxygen-content and low mass; **c** non oxygen-content. Vertical dash dot line indicates the auto-ignition temperature

Results shows important differences in the TG and DSC curves as function of the mass, heating rate and atmosphere. During the mass loss process under an oxidative atmosphere, the higher mass samples seem to have two main slopes during the decomposition process. The first decomposition reaction goes from the initial mass to around the 7.5% of the initial mass, and the second reaction leaves only a 2% of the initial sample mass. For the low mass samples, three main steps can be appreciated: first stage, where the sample loss its mass faster than in the higher sample mass cases; second stage, when the mass is approximately the 50% of the initial mass, the curve changes its slope until around the 15% of the initial mass; and finally, there is another decrease of the mass loss rate until the end of the process. For the fastest heating rate, 50 K·min⁻¹, both samples, high and low mass show a change in its decomposition behaviour. As Fig. 1a shows, the higher sample mass test decreases the two main decomposition process slopes to only one decomposition process slope. According to the lower sample mass test, same effect occurs, decreasing from three to two decomposition process slopes, when the 50 K·min⁻¹ is used. The samples begin to loss their mass at its onset temperature (287 °C, 274 °C, 304 °C,

289 °C, 368 °C and 331 °C for test #1, #2, #3, #4, #6 and #7, respectively), prior to ignition temperature, however, it can be seen that most decomposition process occurs at temperatures higher than the auto-ignition one. As the heating rate increases its value, the onset temperature of the processes increase. The final mass for these tests, from 10 K·min⁻¹ to 50 K·min⁻¹ are: 1.61%, 0.82%, and 0.62% for high mass and 6.87%, 12.27% and 1.50% for low mass.

For the non-oxygen content atmosphere tests, the mass loss rates have a similar shape between heating rates, but the TG curve under 50 K·min⁻¹ heating rate is displaced few degrees to higher temperatures. Both presents one slope once the mass loss process starts up to the end of the process. They have different onset temperature, 407 °C for the slowest heating rate and 418 °C for the fastest heating rate. For these tests, the final mass are 0.82% for 10 K·min⁻¹ test and 0.84% for the 50 K·min⁻¹ test.

DSC results show exothermic character of all reactions under the oxidative atmosphere, with the exception of the high mass sample under the heating rate of 50 K·min⁻¹, that alternates exothermic and endothermic stages. For the oxygen content atmosphere tests, up to 300 °C, DSC curves

have similar values, close to zero. Once the sample begins to lose its mass, the first part of the DSC curve, up to 370 °C approximately, is similar for both types of sample and heating rates. From this point, differences arise based on the amount of mass and heating rate. Whereas for lower mass and all heating rates, there is one high peak of energy released for the first decomposition stage and after the peak, the DSC decreases quickly and there are lower values of DSC for the following stages of the mass loss process. For the larger mass tests, two types of DSC curve shapes are observed. For the 10 K·min⁻¹ and 20 K·min⁻¹, once the first DSC peak is reached, the values of the DSC curves decrease slowly, up to the end of the mass loss process, when the DSC values decrease quickly. Nevertheless, for the higher heating rate, we can see an alternation between exothermic and endothermic reactions. An initial exothermic reaction is followed by a sharp endothermic one, to end with a final exothermic reaction. The more initial mass used, the more DSC peak value obtained, e.g., for 10 K·min⁻¹ are 109.34 mW and 51.80 mW for high and low mass sample, respectively, and for the 20 K·min⁻¹ are 132.36 mW and 57.20 mW, respectively. Nonetheless, for the 50 K·min⁻¹ heating rate, remarkable differences are found based on the initial amount of mass. For the low mass sample test, the process is completely exothermic, with one peak of 126.04 mW. However, the higher sample mass test presents a completely different behaviour. The DSC curve has an exothermic stage from 274 °C up to 429 °C where the DSC peak is produced (215.76 mW). After this peak, there is a remarkable endothermic peak at 497 °C (-215.90 mW), which is not present for the rest of the test, and finally, there is a second exothermic peak at 518 °C (166.66 mW). As far as total energy released is concerned, increasing the heating rate and highest sample mass make the total energy released decrease. For the non-oxygen content atmosphere tests, due to the lack of oxygen, the DSC curves are completely different in comparison with its equivalent with oxygen content atmosphere test. For instance, the mass loss process produces one endothermic DSC peak

instead of exothermic, in other words, the decomposition process absorbs energy from the furnace atmosphere. The total energy absorbed during mass loss processes decreases as the heating rate increases. Next Table 2 summarizes the values of the LLDPE tests shown in previous Fig. 1 during mass loss process.

Figure 2 presents the results of the temperature curves: $(T_{\text{fur}} - T_{\text{sam}})$ (temperature lag) (dotted lines) and $(T_{\text{pro}} - T_{\text{sam}})$ (solid lines) versus the T_{pro} . The vertical dash dot line indicates the LLDPE auto-ignition temperature, 350 °C.

All $(T_{\text{fur}} - T_{\text{sam}})$ and $(T_{\text{pro}} - T_{\text{sam}})$ curves present the next similarities for the initial stages, before the mass begins to decrease: the differences between $(T_{\text{fur}} - T_{\text{sam}})$ increase up to a maximum, and after this maximum value, the curves tend to decrease stabilizing the difference between the T_{sam} and T_{fur} . For the $(T_{\text{pro}} - T_{\text{sam}})$ curve, an initial peak is also produced, and after, the curves stabilize surrounding zero value.

First row of the Fig. 2 shows the $(T_{\text{fur}} - T_{\text{sam}})$ curves. For the oxygen-content atmosphere tests, after the initial peaks there are some alterations when the mass loss processes take place. These alterations, more notable for the high mass tests and fastest heating rates, implies that the progressive approach between T_{fur} and T_{sam} curves has undergone a modification in their tendency.

Next Table 3 shows the temperatures where the deviation peaks are produced and the values of these deviations for the mass loss process. The deviation values are calculated as the difference of the $(T_{\text{fur}} - T_{\text{sam}})$ curve at the temperature of the deviation minus the value that the $(T_{\text{fur}} - T_{\text{sam}})$ curve would have if this curve would remain without any variation. For low sample mass tests, there is only one peak produced with less temperature deviation value in comparison with its equivalent test for high value tests. The values of the deviation increase when the heating rate increases. However, for high sample mass tests, for 20 and 50 K·min⁻¹ heating rate, up to two peaks are produced in each test, one obtaining negative values of the curve $(T_{\text{fur}} - T_{\text{sam}})$ and another with

Table 2 LLDPE. Values of the TG and DSC curves at different heating rates during the mass loss process

Test	Mass/ mg	O ₂ / %	HR/ K·min ⁻¹	Onset/°C	Final mass/%	pDSC/mW	Temp. pDSC/°C	Energy released- absorbed/mJ
#1	11.849	20	10	287	1.61	109.34	388	75,365
#2	1.288	20	10	274	6.87	51.80	375	16,252
#3	26.878	0	10	407	0.82	-31,18	484	-6579
#4	12.514	20	20	304	0.00	132.36	416	53,334
#5	1.110	20	20	289	12.27	57.20	390	12,321
#6	11.763	20	50	368	0.62	215.76/-215.90/166.66	427/496/518	19,896
#7	1.198	20	50	331	1.50	126.04	433	12,801
#8	11.584	0	50	418	0.84	-46.76	517	-3573

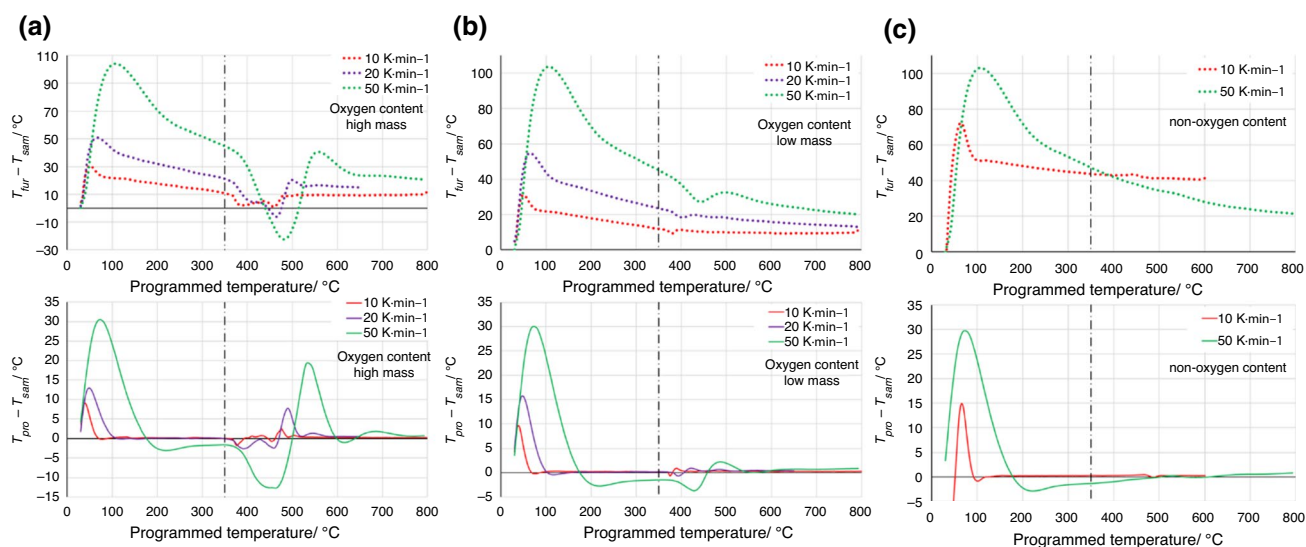


Fig. 2 LLDPE. Comparison ($T_{fur} - T_{sam}$) (temperature lag)(dotted lines) and ($T_{pro} - T_{sam}$) (solid lines) at different heating rates: **a** oxygen-content and high mass; **b** oxygen-content and low mass; **c** non oxygen-content. Vertical dash dot line indicates the auto-ignition temperature

Table 3 Deviations for ($T_{fur} - T_{sam}$) curves of oxygen content atmosphere tests of LLDPE

Test	Initial mass/mg	HR/K·min ⁻¹	Temp. of deviation peak(s)/°C	Peak of deviation value/°C
#1	11.849	10	461	8.48
#2	1.288	10	378	2.15
#4	12.514	20	465–500	22.16–4.04
#5	1.110	20	405	2.37
#6	11.763	50	480–567.5	52.55–13.6
#7	1.198	50	442.5	8.51

positive values. For these both heating rates, the negative values for the curves are between 450 °C and 480 °C for 20 K·min⁻¹, and 440 °C and 515 °C for 50 K·min⁻¹. These negative values imply that sample is hotter than furnace. For non-oxygen content atmosphere tests, the alterations of the curve are minimal, and they are produced approximately 40 °C before of the DSC peak is produced. For instance, for 10 K·min⁻¹ the deviation is produced at 448 °C with a value of 0.2 °C and for 50 K·min⁻¹ is produced at 555 °C with a value of 0.06 °C.

Second row of the Fig. 2 represents the difference between the ($T_{pro} - T_{sam}$) curves and indicates how the sample follows the heating temperature programmed. Whether this difference is similar to zero, the sample is heated according to programmed temperature predefined by the user previously. For oxygen content atmosphere tests and heating rates of 10 and 20 K·min⁻¹, we can appreciate that the curves are similar to zero after the initial peak, and before the samples start to lose their mass. When the mass loss process begins,

the deviations of the curve starts to be appreciable. These deviations are greater when the initial mass and the heating rates increase their values. For instance, at 10 K·min⁻¹ with a low initial mass, the highest deviation peak is 0.77 °C produced at 393 °C, whereas for 20 K·min⁻¹ with a high mass, the highest deviation has a value of 11.40 °C produced at 485 °C. The results for the fastest heating rate (50 K·min⁻¹) displays a slightly different behaviour. After the initial peak, the curves (for both types of initial mass) do not reach a value similar to zero, as the other samples do, before the decomposition process begins. The feature that these curves have in common with the other heating rates is the production of alterations when the mass loss process starts. In these cases, the values are even greater, e.g., for the high mass, the highest peaks are produced at 542.5 °C with a deviation of 18.66 °C and for the low mass is produced at 430 °C with a value of -3.66 °C.

For non-oxygen content atmosphere tests, unlike oxygen content tests, there are not outstanding alterations during the mass loss process. For the 10 K·min⁻¹ test, the ($T_{pro} - T_{sam}$) curve establishes with values surrounding to zero and remains close to zero during the mass loss process. Nonetheless, under a heating rate of 50 K·min⁻¹, ($T_{pro} - T_{sam}$) curve does not achieve zero values prior to the mass loss process starts, and when it begins, both temperatures becomes similar once the mass loss process is almost over.

PMMA

Figure 3 shows the PMMA TG and DSC curves as a function of the T_{sam} . The vertical dash dot line indicates also the PMMA auto-ignition temperature established at 380 °C.

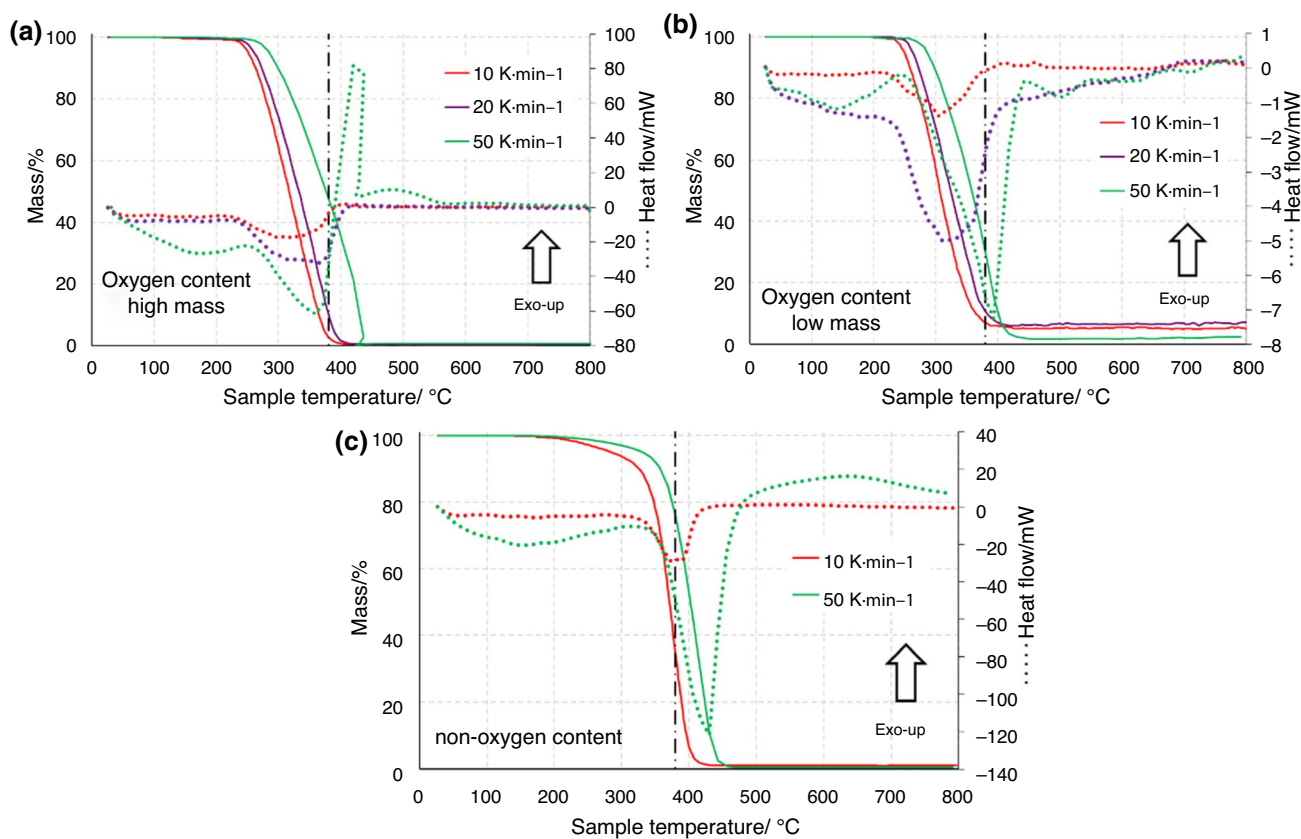


Fig. 3 PMMA. Comparison TG and DSC curves at different heating rates: **a** oxygen-content and high mass; **b** oxygen-content and low mass; **c** non oxygen-content. Vertical dash dot line indicates the auto-ignition temperature

For this polymer, in oxygen content atmosphere tests, up to $20 \text{ K}\cdot\text{min}^{-1}$, small differences arise whether high or low mass is used in TG curves. A very similar onset temperatures are found for the same heating rate tests, e.g., for $10 \text{ K}\cdot\text{min}^{-1}$, the onset temperatures are $244 \text{ }^\circ\text{C}$ and $242 \text{ }^\circ\text{C}$ for high and low mass test, respectively, and for $20 \text{ K}\cdot\text{min}^{-1}$, $254 \text{ }^\circ\text{C}$ and $251 \text{ }^\circ\text{C}$ for high and low mass test, respectively. A slightly higher mass loss rate is found in the lower sample mass test, and the final amount of mass is lower for the high mass tests. In both cases, only one main slope is observed during the whole mass loss process. For these 4 tests, most of the decomposition process take place prior to the auto-ignition temperature, and when the $380 \text{ }^\circ\text{C}$ is reached, the remaining mass for the samples are (high and low mass, respectively): for $10 \text{ K}\cdot\text{min}^{-1}$ $2,86\%$ and $7,08\%$; and for $20 \text{ K}\cdot\text{min}^{-1}$ $10,01\%$ and $10,83\%$. For the DSC curves, as it is evaluated the total heat flow, some differences come from the initial amount of mass, i.e., those tests with high mass and fastest heating rates, produces highest endothermic peaks. At $10 \text{ K}\cdot\text{min}^{-1}$, the DSC peak values are -1.38 mW and -17.39 mW for the low and high sample mass respectively and at $20 \text{ K}\cdot\text{min}^{-1}$, the DSC peak values are -5.01 mW and -31.98 mW for the low and high sample

mass, respectively. Although these peak values seem to be nothing alike, if they are normalized by their sample mass, they become more similar. For $10 \text{ K}\cdot\text{min}^{-1}$, the values are $-1.16 \text{ mW}\cdot\text{mg}^{-1}$ and $-0.91 \text{ mW}\cdot\text{mg}^{-1}$ for low and high mass, respectively, and for the heating rate of $20 \text{ K}\cdot\text{min}^{-1}$, these values are $-3.80 \text{ mW}\cdot\text{mg}^{-1}$ and $-2.02 \text{ mW}\cdot\text{mg}^{-1}$ for low and high sample mass, respectively. During the decomposition process of these tests, the total balance of energy is negative, i.e., the reactions produced absorb energy to take place. As the initial sample mass is lower, less energy is absorbed.

Nevertheless, at the heating rate of $50 \text{ K}\cdot\text{min}^{-1}$, TG curve reflects visible differences between high and low mass sample tests. Although both tests start to lose their mass at similar temperatures ($284 \text{ }^\circ\text{C}$ for the high mass test and $269 \text{ }^\circ\text{C}$ for low mass test), at $300 \text{ }^\circ\text{C}$ the TG curves begins the differences. For low mass test, the TG curve is similar to a straight line during the mass loss process up to its end. However, for the high mass test, the TG curve has a particular shape at the end of the mass loss process. The mass loss process finished in a sharp way, i.e., between $428 \text{ }^\circ\text{C}$ and $438 \text{ }^\circ\text{C}$, producing in these points the particular feature that for one sample temperature two mass values are available. The DSC curves present also some differences. On the one

hand, up to 390 °C approximately both curves are endothermic with endothermic peaks -61.40 mW and -7.25 mW for high and low mass, respectively (-3.97 mW·mg⁻¹ and -6.34 mW·mg⁻¹, respectively). On the other hand, after auto-ignition temperature (380 °C), the low mass test remains its endothermic character; however, the high mass test shows a remarkable exothermic peak, with a value of 81.68 mW at 419 °C. The DSC curve after this exothermic peak produces a sudden decrease up to 6.06 mW, and then, the DSC values decreases slowly up to the mass loss process ends. These different behaviours are reflected in the total balance of energy of the processes. Whereas for the high initial mass is required -1278 mJ (-76.5 J·g⁻¹) to the decomposition process occurs, when the initial sample mass is low, it requires -681 mJ (-596 J·g⁻¹).

For non-oxygen content atmosphere tests, TG curves follow the expected behaviour, with the one corresponding to fastest heating rate displaced to higher temperatures. Same

circumstance is produced with the DSC curve, where both curves are similar in shape, presenting an endothermic peak during the mass loss process, but with different values. The heating rate of 10 K·min⁻¹ has a peak of -29.01 mW (-1.67 mW·mg⁻¹) produced at 374 °C, and the fastest heating rate produced an endothermic peak of -121.47 mW (-8.04 mW·mg⁻¹) at 430 °C. For this heating rate, once the mass loss process is finished, the DSC curve increases up to 16.60 mW at 629 °C. The onset temperatures for these tests are 231 °C for 10 K·min⁻¹ and 255 °C for 50 K·min⁻¹. Despite the different the heating rates employed, similar amounts of energy are absorbed by the samples, -9322 mJ for 10 K·min⁻¹ and -9127 mJ for the 50 K·min⁻¹. Next Table 4 gathers the values of the PMMA tests showed in previous Fig. 3 during the thermal decomposition process.

Figure 4 displays the temperature curves for the PMMA tests: ($T_{\text{fur}} - T_{\text{sam}}$) (temperature lag)(dotted lines) and ($T_{\text{pro}} - T_{\text{sam}}$) (solid lines) versus the T_{pro} . The vertical dash

Table 4 PMMA. Values of the TG and DSC curves at different heating rates during the mass loss process

Test	Mass/ mg	O ₂ / %	HR/ K·min ⁻¹	Onset/°C	Final mass/%	pDSC/mW	Temp. pDSC/°C	Energy released/ absorbed/mJ
#9	19.019	20	10	244	0.46	-17.39	299	-10,618
#10	1.193	20	10	242	4.94	-1.38	304	-702
#11	17.362	0	10	192	0.94	-29.01	374	-9322
#12	15.794	20	20	254	0.38	-31.98	364	-10,234
#13	1.318	20	20	251	5.93	-5.01	314	-1259
#14	15.599	20	50	284	0.35	-61.40/81.61	359/419	-1278
#15	1.143	20	50	269	1.66	-7.25	393	-681
#16	15.097	0	50	214	0.41	-121.47	430	-9127

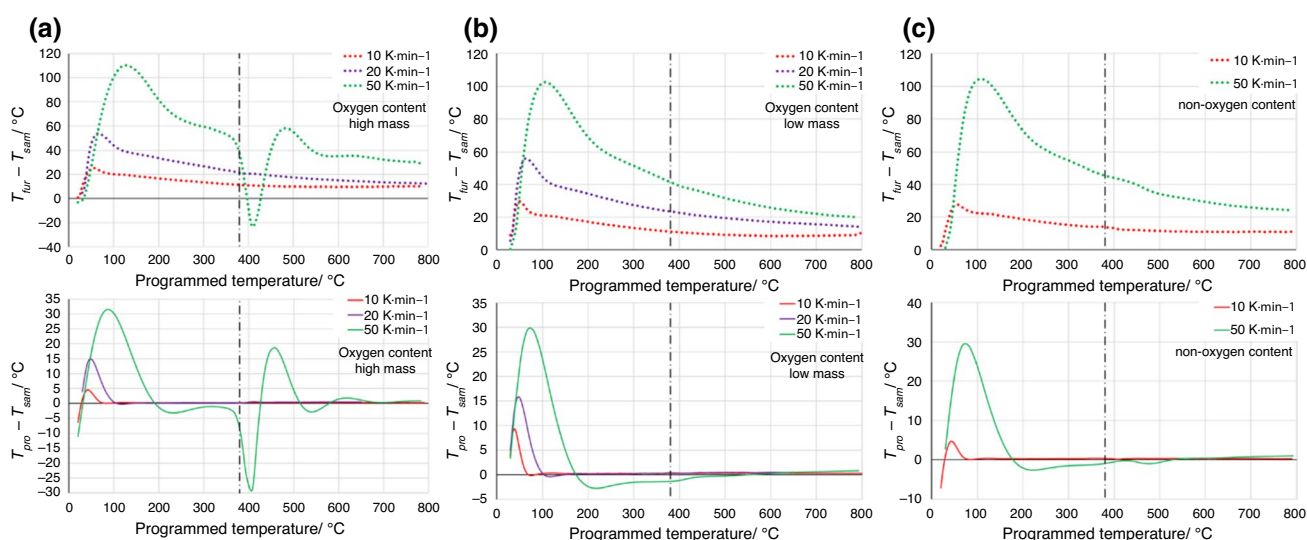


Fig. 4 PMMA. Comparison ($T_{\text{fur}} - T_{\text{sam}}$) (temperature lag)(dotted lines) and ($T_{\text{pro}} - T_{\text{sam}}$) (solid lines) at different heating rates: **a** oxygen-content and high mass; **b** oxygen-content and low mass; **c** non oxygen-content. Vertical dash dot line indicates the auto-ignition temperature

dot line indicates the PMMA auto-ignition temperature, 380 °C.

As the curves showed previously for the LLDPE, both $(T_{\text{fur}} - T_{\text{sam}})$ and $(T_{\text{pro}} - T_{\text{sam}})$ curves have the same features for the initial stages of the process, prior to the sample begins to loss its mass. In other words, the differences between $(T_{\text{fur}} - T_{\text{sam}})$ curve increases up to a maximum value, and then, it decreases up to stabilizing the differences between the T_{sam} and T_{fur} . As far as $(T_{\text{pro}} - T_{\text{sam}})$ curves are concern, an initial peak is also produced, but after it, the curve should tends values similar to zero before the sample begins to loss its mass. However, for the fastest heating rate (green solid curves of Fig. 4), the curves do not stabilise around zero value, but a value close to zero.

The upper row of the Fig. 4 displays the $(T_{\text{fur}} - T_{\text{sam}})$ curves. It can be seen in both sample masses that for the oxygen content atmosphere tests under the heating rates of 10 and 20 K·min⁻¹, there are no alterations in the $(T_{\text{fur}} - T_{\text{sam}})$ curve once the mass loss process begins. It implies that for whole test, the sample follows the T_{fur} , with a certain degree of delay, even when the mass loss process takes place. This feature is reflected in the $(T_{\text{pro}} - T_{\text{sam}})$ curves (lower row of Fig. 4). After the initial temperature deviation peak, the $T_{\text{pro}} - T_{\text{sam}}$ value decrease to close to zero values. However, this behaviour is not presented for the 50 K·min⁻¹ heating rate test. For the fastest heating rate, the $(T_{\text{fur}} - T_{\text{sam}})$ curve undergoes large variations, producing two deviation peaks at 407,5 °C and 482,5 °C with values of 68.65 °C and 19.27 °C respectively (compared with the values if this curve would continue without alterations). Besides, this curve has negative values between 397 °C and 429 °C showing that the furnace temperature is cooler than the sample one. It means that for this range of temperatures, the sample remains hotter than the furnace. The $(T_{\text{pro}} - T_{\text{sam}})$ curve reflexes previous feature and it presents non-zero values during almost mass loss process. There are two peaks at 407.5 °C and at 457.5 °C, with values of -28.81 °C and 18.75 °C respectively.

For non-oxygen atmosphere content tests, the slowest heating rate shows a behaviour similar to its equivalent test in oxygen content atmosphere, i.e., there is no appreciable alterations for the $(T_{\text{fur}} - T_{\text{sam}})$ curve during the mass loss process, but small deviation at 374 °C of 0.02 °C. The $(T_{\text{pro}} - T_{\text{sam}})$ curve remains close to zero values during the mass loss process. The fastest heating rate has slightly different behaviour. The deviation of the $(T_{\text{fur}} - T_{\text{sam}})$ curve is more significant than the slowest heating rate. At the temperature of the DSC peak, 430 °C approximately, there is a deviation of 0.82 °C. Although the value of the deviation is much smaller than the equivalent test in oxygen content atmosphere, the $(T_{\text{pro}} - T_{\text{sam}})$ curve is not able to stabilize around zero values.

Discussions

LLDPE

The obtained TG curves agrees with other work available in literature under similar boundary conditions: [35, 36] for 10 K·min⁻¹, [37] for 20 K·min⁻¹ both for oxygen content atmosphere tests and [36, 38] for 10 K·min⁻¹ for non-oxygen content atmosphere. As far as TG and DSC results show, the oxygen concentration, initial amount of mass and the heating rate strongly influence the LLDPE decomposition process. For instance, the onset temperature of the process decrease when the oxygen concentration increases, and faster heating rates delay the onset temperature, i.e., it makes that decomposition process takes place at higher temperatures [12, 21, 34]. If the amount of sample mass decreases, the decomposition process takes place at lower temperatures. These features can be appreciated in Fig. 1, where TG and DSC curves for the LLDPE curves are shown.

For the LLDPE, all samples loss most of their mass after the auto-ignition temperature of the material is passed (Fig. 1). This feature eases the possibility of the auto-ignition of the gases released at the auto-ignition temperature, and therefore, the combustion reactions of the polymer could be analysed. This can be seen in the exothermic reactions obtained in the thermal decomposition of the LLDPE under an oxidative atmosphere (Fig. 1). The auto-ignition of the material means the auto-ignition of their pyrolysates. It depends on several factors [24], among them, the molecular structure, fuel concentration, pressure and flow velocity and turbulence. The TG and DSC sample mass is directly related with the fuel concentration available when the auto-ignition threshold is reached. The more sample mass, the more fuel available when the auto-ignition threshold is passed. Fuel concentration also affect to the heat flow, as a large amount of fuel produces a large heat release, if there is enough oxygen available.

According to the DSC results, it is appreciated an endothermic peak during the thermal decomposition process in the test with the higher sample mass and the heating rate of 50 K·min⁻¹. This peak lacks of physical meaning in the middle of the LLDPE combustion reaction. The appearance of this endothermic peak may be explained by the following sequence of events. The large amount of sample mass of this test, that implies a large fuel concentration when decomposition begins, linked with the large heating rate, that implies a large fuel flow velocity, produce a first exothermic reaction peak with a large amount of heat released (223.94 mW). This exothermic reaction produces a substantial increase of the T_{sam} , greater than the T_{fur} and the T_{pro} for that moment (Fig. 2a). As a result of

this increase, the furnace tries to decrease the T_{sam} to the T_{pro} . This forces the T_{fur} to decrease its temperature below the T_{sam} . By the time the heat flow released by the sample decreases, the T_{sam} is higher than the T_{fur} , i.e., the sample hotter than the furnace. In this case, the sample is cooled by the furnace, due to the unusual deviation of its temperature, which for the internal calculations of the DSC equipment represent an endothermic reaction (sample is cooling). Accordingly, the DSC has negative values, producing the endothermic peak. Afterwards, and once again, the T_{fur} pass the T_{sam} , returning back the initial situation, where the T_{sam} is lower than T_{fur} , resuming the mass loss process and releasing the energy, as the second DSC peak indicates.

As it is quoted previously [24], the factors that determines the amount of pyrolysates, such as fuel concentration and flow velocity, are mainly determined by the amount of mass loss and the mass loss rate. To verify whether there are some evidences when the T_{fur} and T_{sam} starts to deviate, next Table 5 gathers, at the temperature when the deviation starts (Fig. 2), the values of the MLR, and remaining mass.

The faster heating rates and lower initial mass produce that the deviation takes place at higher temperatures. The MLR, when the deviation starts, increases when the initial mass is higher and the heating rate is faster. Moreover, the remaining mass when the deviation starts is larger when the initial mass is higher. Finally, for the non-oxygen content atmosphere tests, despite the lack of oxygen avoids any combustion reaction, it is observed that a heating rate of $50 \text{ K}\cdot\text{min}^{-1}$ makes that T_{sam} are not similar to the T_{pro} , producing values different to zero. This deviation could be explained by the fact of the heat absorption of the material is limited by the heat capacity and the apparition of the temperature lag phenomenon quoted previously [1]. Hence, if the heating rate is high, the heat flow transferred to the sample should be minimized by limiting the initial amount of mass [1, 39].

PMMA

In the case of the PMMA, the obtained TG and DSC curves agrees with executed tests using similar boundary conditions alike this work such as such as [40–42] for oxygen content atmosphere and [41–43] for non-oxygen content atmosphere tests. As it was quoted above [12, 21, 34], lower sample mass and slower heating rates lead to decrease the onset temperature of the process (Fig. 3).

For this polymer, the most part of the mass loss process takes place prior to the auto-ignition temperature ($380 \text{ }^\circ\text{C}$) as Fig. 3 shows. This fact produces endothermic decomposition reactions, although PMMA it is known to be a polymer that releases an important amount of energy. Only when the heating rate is $50 \text{ K}\cdot\text{min}^{-1}$ and the initial sample mass is high, an event of auto-ignition seems to takes place (Fig. 3a) producing an exothermic decomposition reaction that modifies the both TG and DSC curve. This exothermic reaction is caused by the ignition of the gases released from the decomposition at higher temperatures than the auto-ignition one. In order to analyse the relation between the auto-ignition temperature and the conditions of the sample to ignite, Table 6 gathers, for the oxygen content atmosphere PMMA tests, the onset temperatures, and the remaining mass and MLR at auto-ignition temperature.

According Table 6, the onset temperatures are considerably lower than the auto-ignition temperature. This circumstance makes that for slower heating rates (10 and $20 \text{ K}\cdot\text{min}^{-1}$) the most amount of mass is loss at cooler temperatures than the auto-ignition one. Therefore, when this temperature is reached the remaining amount of mass and the MLR, which are related with the fuel concentration and the flow velocity, are insignificant. Hence, the small concentration of pyrolysates or its lack prevents the auto-ignition event. Nevertheless, at $50 \text{ K}\cdot\text{min}^{-1}$ there is a considerable amount of mass remaining for both tests when the auto-ignition threshold is achieved. On the one hand, for the high mass, there is 47.67% of remaining mass which combined with the mass loss rate ($-1.2\text{E-}1 \text{ mg}\cdot\text{s}^{-1}$) appears to

Table 5 Measurements for oxygen content atmosphere LLDPE tests when the deviation of the temperature curves starts

Test	Initial mass/mg	HR/ $\text{K}\cdot\text{min}^{-1}$	Temp. deviation starts/ $^\circ\text{C}$	Data measured at T. deviation starts	
				MLR/ $\text{mg}\cdot\text{s}^{-1}$	Remaining mass/%
#1	11.849	10	340	$-2.3\text{E}-03$	96.9
#2	1.288	10	365	$-1.1\text{E}-03$	79.5
#4	12.514	20	350	$-2.9\text{E}-03$	98.1
#5	1.110	20	370	$-1.5\text{E}-03$	91.5
#6	11.763	50	360	$-5.4\text{E}-03$	98.4
#7	1.198	50	380	$-5.2\text{E}-03$	93.5

Table 6 Onset temperatures and remaining mass at auto-ignition temperatures for oxygen content atmosphere PMMA tests

Test	Initial mass/mg	HR/K·min ⁻¹	Onset temperature/°C	Data measured at auto-ignition temperature	
				MLR/mg·s ⁻¹	Remaining mass/%
#9	19.019	10	244	- 6.7E- 03	2.89
#10	1.193	10	242	- 1.9E- 04	7.08
#12	15.794	20	254	- 3.3E- 02	10.01
#13	1.318	20	251	- 1.2E- 03	10.81
#14	15.559	50	284	- 1.2E- 01	47.67
#15	1.143	50	269	- 9.9E- 03	28.26

be sufficient to trigger an auto-ignition event, producing a large DSC exothermic peak (81.61 mW). On the other hand, for the low mass, there is a 28.26% of remaining mass, with a mass loss rate of $-9.9\text{E}-03\text{ mg}\cdot\text{s}^{-1}$, which seems to be not sufficient to trigger the auto-ignition, not producing a prominent exothermic DSC peak, as previous Fig. 3 displays.

Furthermore, as previously stated, the high mass test for the fastest heating rate presents a particularity on the TG curve at the end of mass loss process because this process finishes in a sharp way (between 418 °C and 428 °C). It can be observed that the sample temperature decreases during the mass loss process, producing between these temperatures the particular feature that two mass values correspond to one sample temperature. This feature indicates that experimental conditions are far from desired. This particular behaviour and shape for the TG curves can be also appreciated in the work of [22], where the samples analysed under oxidative atmosphere shown a similar behaviour in their TG curves shape. Same TG curves shape are found in. Same TG curves shape are found in [23]. Here, the authors associate this effect, for the corn stover, to the self-heating event when the samples are tested under oxygen-atmosphere. The authors attribute the difference between atmospheres to the apparition of pyrolysis and combustion processes for the oxidative atmosphere and pyrolysis process uniquely for non-oxidative atmosphere.

The particular behaviour observed for the high mass test at $50\text{ K}\cdot\text{min}^{-1}$ in oxygen content atmosphere is reflected in the temperature curves of the Fig. 4. Whereas for oxygen content atmosphere tests and low mass any variation is appreciated during the mass loss process in ($T_{\text{fur}} - T_{\text{sam}}$) curve (dotted lines), even for the fastest heating rate (Fig. 4b), a considerable variation of the ($T_{\text{fur}} - T_{\text{sam}}$) curve appears at the heating rate of $50\text{ K}\cdot\text{min}^{-1}$ (Fig. 4a). Two deviation peaks appear at 407 °C and 482 °C, with values of -26.51 °C and 63.76 °C respectively. Furthermore, this curve has negative values between 390 °C and 428 °C, i.e. T_{sam} is hotter than T_{fur} . This circumstance was also observed in the LLDPE test with the same boundary conditions, and

it is associated with the self-heating effect of the studied polymers that, due to the amount of heat released during their combustion forces the testing apparatus to compensate the rising of the temperatures. Accordingly, the furnace temperature decreases affecting the results.

Analysing the ($T_{\text{pro}} - T_{\text{sam}}$) curves, the fastest heating rate and high mass (oxygen content atmosphere test) shows two deviation peaks at 407 °C and 457 °C with a values of 20.65 °C and 23.54 °C. The rest of the test under 10 and 20 $\text{K}\cdot\text{min}^{-1}$, show how during the mass loss process the curve remains with values close to zero. However, as it was also appreciated in the LLDPE test, the fastest heating rate produces that T_{sam} are not similar to T_{pro} , even when the auto-ignition is not produced. This circumstance is observed in the $50\text{ K}\cdot\text{min}^{-1}$ test for low mass in oxygen content atmosphere and in $50\text{ K}\cdot\text{min}^{-1}$ test under non-oxygen content atmosphere.

Conclusions

This work aims to analyse the self-heating influence in the thermal decomposition processes of two widely used polymers as PMMA and LLDPE. TG/DSC test are used to evaluate the thermal decomposition processes. Boundary conditions of the tests definition as sample mass, atmospheres, and heating rate are considered to evaluate its influence on the polymers self-heating effect on the thermal decomposition. To assess the influence of the boundary conditions we monitor, besides TG and DSC curves, temperature of the tested sample and furnace. Both temperatures, in combination with the pre-programed one, allow obtaining two curves: ($T_{\text{fur}} - T_{\text{sam}}$) and ($T_{\text{pro}} - T_{\text{sam}}$). These curves are useful to display: whether the sample T_{sam} follows the T_{fur} , with a certain constant delay during the mass loss process; and any alteration in the tendency of the curves due to the heat release produced by the self-heating. To fulfil the aim, several STA tests to LLDPE and PMMA samples were carried out modifying their initial mass and testing them under three

heating rates (10, 20 and 50 K·min⁻¹) and two atmospheres (oxygen and non-oxygen content).

In the light of the obtained results, we can outline next conclusions.

- For non-oxygen content atmosphere, the heating rate seems to have small relevance on the shape TG and DSC curves, which agrees with [22, 23]. The differences between T_{sam} and T_{pro} are found at the beginning of the experimental tests. The heating rate of 50 K·min⁻¹ produces temperature deviations of around 30 °C in both polymers when the T_{pro} is lower than 200 °C, whereas for a heating rate of 10 K·min⁻¹, the temperature deviations are lower than 15 °C, for both polymers, when the T_{pro} is lower than 100 °C. It is highly recommended to check temperature deviations while the thermal decomposition is analysed at low temperatures with high heating rates. It is recommended the employ of the slow heating rates in order to minimize the effects of the sample temperature lag [1, 39] that could prevent the T_{sam} reproduces correctly the T_{pro} .
- Under oxygen content atmosphere, both the initial amount of sample mass and heating rate may produce variations on the T_{sam} and T_{fur} curves. The degree and range of these variations depends on several factors. Fastest heating rates and heavier initial sample mass produces that decomposition process takes place at higher temperatures. The auto-ignition temperature of the material plays a key role. If the mass loss process or a large part of it takes place at temperatures over the auto-ignition one, the auto-combustion event is highly likely, as the LLDPE tests. This allows analysing combustion reactions on the TG/DSC. However, if the mass loss process or a great part of it, is produced at cooler temperatures than the auto-ignition temperature, combustion will not take place and cannot be studied with the TG/DSC. As in the case of the non-oxygen atmosphere analysis, the initial amount of mass has less influence in the decomposition process. The auto-ignition temperature threshold modifies the character of the DSC. If the mass loss process takes place over this temperature, the endothermic character of the process for the earlier stages could change to exothermic, as the PMMA case. This complicates the analysis of PMMA combustion reactions with the TG/DSC test. Nevertheless, increasing the sample mass and the heating rate, the PMMA mass loss process moves closer to the auto-ignition temperature threshold, easing the conditions inside the furnace to trigger the auto-combustion event. Nonetheless, these boundary conditions produce a high self-heating, due to the appearance of the combustion energy of the pyrolysates gases, and the temperature lag undergoes variations during the mass loss process. Accordingly, the TG and DSC curves modify

their shape and values. In some cases, the self-heating phenomenon has such a large influence that TG curve is modified coming up several values of the sample mass (or equivalent extent of conversion) for a single value of temperature, in accordance with shown in [22, 23]. The magnitude of self-heating effect not only depends on the character of the material but also on the selected boundary conditions.

- To avoid the self-heating process or minimize it, it is recommended the employ of low mass for the samples and slow heating rates. In this work, the samples about 1 mg seem to be less affected by auto-combustion events or reduce its effects. If it is possible, when an oxygen content atmosphere is used, we recommend to check material auto-ignition temperature, for a better understanding of the material behaviour and TG/DSC results.
- This paper highlights the importance of checking the TG/DSC test boundary conditions by monitoring the temperature curves ($T_{\text{fur}} - T_{\text{sam}}$) and ($T_{\text{pro}} - T_{\text{sam}}$). The authors recommend verify these temperatures curves for each test, since the comparison of these curves allows the researcher to accept or discard not enough accurate results or testing the material under other boundary conditions, avoiding the auto-combustion events and the consequences of the self-heating. The recommendations indicated in [1] about how to avoid self-heating events are prescribed taking into account hazardous materials. Although the analysed polymers in the present work cannot be included in this class, under certain conditions self-heating event can emerge during the test. Nevertheless, there are some works in literature such as [14, 15], that even testing materials at elevated heating rates that could lead to ease self-heating events, the TG curves obtained do not show any unusual modification behaviour as shown in Fig. 3 and in [22, 23], stressing the importance of checking the temperature curves.

Acknowledgements This work has been previously presented in 17th International Congress on Thermal Analysis and Calorimetry (ICTAC2020). The authors are grateful to the organization for their collaboration. This publication is part of the R&D project RTC-2017-6066-8 funded by MCIN/ AEI/10.13039/501100011033/ and ERDF “Una manera de hacer Europa”. The authors would like to thank to the Consejo de Seguridad Nuclear for the cooperation and co-financing the project “Metodologías avanzadas de análisis y simulación de escenarios de incendios en centrales nucleares”.

Funding Open Access funding provided thanks to the CRUE-CSIC agreement with Springer Nature.

Open Access This article is licensed under a Creative Commons Attribution 4.0 International License, which permits use, sharing, adaptation, distribution and reproduction in any medium or format, as long as you give appropriate credit to the original author(s) and the source, provide a link to the Creative Commons licence, and indicate if changes

were made. The images or other third party material in this article are included in the article's Creative Commons licence, unless indicated otherwise in a credit line to the material. If material is not included in the article's Creative Commons licence and your intended use is not permitted by statutory regulation or exceeds the permitted use, you will need to obtain permission directly from the copyright holder. To view a copy of this licence, visit <http://creativecommons.org/licenses/by/4.0/>.

References

- Vyazovkin S, Chrissafis K, Di Lorenzo ML, Koga N, Pijolat M, Roduit B, Sbirrazzuoli N, Suñol JJ. ICTAC kinetics committee recommendations for collecting experimental thermal analysis data for kinetic computations. *Thermochim Acta*. 2014;590:1–23. <https://doi.org/10.1016/j.tca.2014.05.036>.
- ISO 11358–1. Plastics—Thermogravimetry (TG) of polymers—Part 1: General principles. ISO. 2014; <https://www.iso.org/standard/59710.html>. Accessed 31 Jan 2022.
- ISO 11357–1. Plastics—Differential scanning calorimetry (DSC)—Part 1: General principles. ISO. 2016; <https://www.iso.org/standard/70024.html>. Accessed 31 Jan 2022.
- Laidler KJ. The development of the Arrhenius equation. *J Chem Educ*. 1984;61(6):494–8. <https://doi.org/10.1021/ed061p494>.
- Sharma A, Mohanty B. Non-isothermal TG/DTG-FTIR kinetic study for devolatilization of Dalbergia sissoo wood under nitrogen atmosphere. *J Therm Anal Calorim*. 2020;146(2):865–79. <https://doi.org/10.1007/s10973-020-09978-0>.
- Gözke G, Açıkalin K. Pyrolysis characteristics and kinetics of sour cherry stalk and flesh via thermogravimetric analysis using iso-conventional methods. *J Therm Anal Calorim*. 2020;146(2):893–910. <https://doi.org/10.1007/s10973-020-10055-9>.
- Lautenberger C, Fernandez-Pello A. Optimization algorithms for material pyrolysis property estimation. *Fire Saf Sci*. 2011;10:751–64. <https://doi.org/10.3801/iafss.fss.10-751>.
- Wrzecień M, Matyszczyk G, Bandzerewicz A, Ruśkowski P, Gadomska-Gajadur A. Kinetics of polycondensation of citric acid with glycerol based on a genetic algorithm. *Org Process Res Dev*. 2021;25(2):271–81. <https://doi.org/10.1021/acs.oprd.0c00492>.
- Alonso A, Lázaro M, Lázaro P, Lázaro D, Alvear D. Assessing the influence of the input variables employed by fire dynamics simulator (FDS) software to model numerically solid-phase pyrolysis of cardboard. *J Therm Anal Calorim*. 2019;140(1):263–73. <https://doi.org/10.1007/s10973-019-08804-6>.
- Korobeinichev OP, Paletsky AA, Gonchikzhapov MB, Glaznev RK, Gerasimov IE, Naganovsky YK, Shundrina IK, Snegirev AY, Vinu R. Kinetics of thermal decomposition of PMMA at different heating rates and in a wide temperature range. *Thermochim Acta*. 2019;671:17–25. <https://doi.org/10.1016/j.tca.2018.10.019>.
- Ferriol M, Gentilhomme A, Cochez M, Oget N, Mieloszynski JL. Thermal degradation of poly(methyl methacrylate) (PMMA): modelling of DTG and TG curves. *Polym Degrad Stab*. 2003;79(2):271–81. [https://doi.org/10.1016/s0141-3910\(02\)00291-4](https://doi.org/10.1016/s0141-3910(02)00291-4).
- Alonso A, Lázaro M, Lázaro P, Lázaro D, Alvear D. LLDPE kinetic properties estimation combining thermogravimetry and differential scanning calorimetry as optimization targets. *J Therm Anal Calorim*. 2019;138(4):2703–13. <https://doi.org/10.1007/s10973-019-08199-4>.
- Cammenga HK, Eysel W, Gmelin E, Hemminger WF, Höhne GW, Sarge SM. The temperature calibration of scanning calorimeters: Part 2. Calibration substances. *Thermochim Acta*. 1993;219:333–42. [https://doi.org/10.1016/0040-6031\(93\)80510-H](https://doi.org/10.1016/0040-6031(93)80510-H).
- Shen DK, Gu S, Luo KH, Bridgwater AV, Fang MX. Kinetic study on thermal decomposition of woods in oxidative environment. *Fuel*. 2009;88(6):1024–30. <https://doi.org/10.1016/j.fuel.2008.10.034>.
- Sittisun P, Tippayawong N, Wattanasiriwech D. Thermal Degradation Characteristics and Kinetics of Oxy Combustion of Corn Residues. *Adv Mater Sci Eng* 2015; Article ID 304395, <https://doi.org/10.1155/2015/304395>
- Blázquez G, Pérez A, Iáñez-Rodríguez I, Martínez-García C, Calero M. Study of the kinetic parameters of thermal and oxidative degradation of various residual materials. *Biomass Bioenergy*. 2019;124:13–24. <https://doi.org/10.1016/j.biombioe.2019.03.008>.
- Gallagher P, Johnson DW Jr. The effects of sample size and heating rate on the kinetics of the thermal decomposition of CaCO₃. *Thermochim Acta*. 1973;6(1):67–83. [https://doi.org/10.1016/0040-6031\(73\)80007-3](https://doi.org/10.1016/0040-6031(73)80007-3).
- Bockhorn H, Hornung A, Hornung U, Jakobströer P. Modelling of isothermal and dynamic pyrolysis of plastics considering non-homogeneous temperature distribution and detailed degradation mechanism. *J Anal Appl Pyrolysis*. 1999;49(1–2):53–74. [https://doi.org/10.1016/s0165-2370\(98\)00130-2](https://doi.org/10.1016/s0165-2370(98)00130-2).
- Ceipidor UB, Bucci R, Magrí AD. Using thermoanalytical data Part 2. The dependence of kinetic data available from thermogravimetry on sample and instrument parameters: a method for calculating “true” kinetic parameters. *Thermochim Acta*. 1990;161(1):37–49. [https://doi.org/10.1016/0040-6031\(90\)80284-6](https://doi.org/10.1016/0040-6031(90)80284-6).
- Armand JY, Vergnaud JM. Effect of the value of heating rate in DSC on the kinetic parameters, when there is high enthalpy of reaction. *Thermochim Acta*. 1988;131:15–27. [https://doi.org/10.1016/0040-6031\(88\)80053-4](https://doi.org/10.1016/0040-6031(88)80053-4).
- Lázaro D, Lázaro M, Alonso A, Lázaro P, Alvear D. Influence of the STA boundary conditions on thermal decomposition of thermoplastic polymers. *J Therm Anal Calorim*. 2019;138(4):2457–68. <https://doi.org/10.1007/s10973-019-08787-4>.
- Jiang L, Yuan X, Li H, Xiao Z, Liang J, Wang H, Zhibin W, Chen X, Zeng G. Pyrolysis and combustion kinetics of sludge–camphor pellet thermal decomposition using thermogravimetric analysis. *Energy Convers Manag*. 2015;2015(106):282–9. <https://doi.org/10.1016/j.enconman.2015.09.046>.
- Conesa JA, Uruña A, Díez D. Corn stover thermal decomposition in pyrolytic and oxidant atmosphere. *J Anal Appl Pyrolysis*. 2014;106:132–7. <https://doi.org/10.1016/j.jaap.2014.01.010>.
- Babrauskas V. *Ignition Handbook: Principles and Applications to Fire Safety Engineering, Fire Investigation, Risk Management and Forensic Science*: Fire Science Publishers; 2003
- Na Y, Dai S, Chen C. Direct synthesis of polar-functionalized linear low-density polyethylene (LLDPE) and low-density polyethylene (LDPE). *Macromolecules*. 2018;51(11):4040–8. <https://doi.org/10.1021/acs.macromol.8b00467>.
- Peterson JD, Vyazovkin S, Wight CA. Kinetics of the thermal and thermo-oxidative degradation of polystyrene, polyethylene and poly (propylene). *Macromol Chem Phys*. 2001;202(6):775–84. [https://doi.org/10.1002/1521-3935\(20010301\)202:6%3c775::AID-MACP775%3e3.0.CO;2-G](https://doi.org/10.1002/1521-3935(20010301)202:6%3c775::AID-MACP775%3e3.0.CO;2-G).
- SFPE Handbook of Fire Protection Engineering. Appendix 3. Hurlley JM, Gottuk D, Hall Jr JR, Harada K, Kuligowski E, Puchovsky M, Torero J, Watts Jr JM, Wieczorek C. Society of Fire Protection Engineers. Springer, New York, NY. 2016 <https://doi.org/10.1007/978-1-4939-2565-0>
- Zaghloul MMY. Mechanical properties of linear low-density polyethylene fire-retarded with melamine polyphosphate. *J Appl Polym Sci*. 2018;135(46):46770. <https://doi.org/10.1002/app.46770>.

29. Materials Handbook. A Concise Desktop Reference. Cardarelli F. Springer, London. 2008. <https://doi.org/10.1007/978-1-84628-669-8>
30. Costache MC, Wang D, Heidecker MJ, Manias E, Wilkie CA. The thermal degradation of poly (methyl methacrylate) nanocomposites with montmorillonite, layered double hydroxides and carbon nanotubes. *Polym Adv Technol.* 2006;17(4):272–80. <https://doi.org/10.1002/pat.697>.
31. SFPE Handbook of Fire Protection Engineering. Chapter 21. Hurlley JM, Gottuk D, Hall Jr JR, Harada K, Kuligowski E, Puchovsky M, Torero J, Watts Jr JM, Wieczorek C. Society of Fire Protection Engineers. Springer, New York, NY. 2016 <https://doi.org/10.1007/978-1-4939-2565-0>
32. Kashiwagi T, Ohlemiller TJ. A study of oxygen effects on non-flaming transient gasification of PMMA and PE during thermal irradiation. In Symposium (International) on Combustion. Elsevier. 1982; 19(1), 815–823. [https://doi.org/10.1016/S0082-0784\(82\)80257-9](https://doi.org/10.1016/S0082-0784(82)80257-9)
33. Comesaña R, Gómez MA, Álvarez MA, Eguía P. Thermal lag analysis on a simulated TGA-DSC device. *Thermochim Acta.* 2012;547:13–21. <https://doi.org/10.1016/j.tca.2012.08.008>.
34. Al-Salem SM, Bumajdad A, Khan AR, Sharma BK, Chandrasekaran SR, Al-Turki FA, Jassem FH, Al-Dhafeeri AT. Non-isothermal degradation kinetics of virgin linear low density polyethylene (LLDPE) and biodegradable polymer blends. *J Polym Res.* 2018;25:111. <https://doi.org/10.1007/s10965-018-1513-7>.
35. Xie R, Qu B. Synergistic effects of expandable graphite with some halogen-free flame retardants in polyolefin blends. *Polym Degrad Stab.* 2001;71(3):375–80. [https://doi.org/10.1016/S0141-3910\(00\)00188-9](https://doi.org/10.1016/S0141-3910(00)00188-9).
36. Khonakdar HA. Dynamic mechanical analysis and thermal properties of LLDPE/EVA/modified silica nanocomposites. *Compos B Eng.* 2015;76:343–53. <https://doi.org/10.1016/j.compositesb.2015.02.031>.
37. Ye W, Du L, Tian X. Synthesis and Properties of a Novel Intumescent Flame Retardant and its Application in LLDPE. *Int Polym Process.* 2014;29(2):191–6. <https://doi.org/10.3139/217.2716>.
38. Sangeetha V, Gopinath D, Prithivirajan R, Chandran VG, Kumar RM. Investigating the mechanical, thermal and melt flow index properties of HNTs–LLDPE nano composites for the applications of rotational moulding. *Polym Test.* 2020;2020(89): 106595. <https://doi.org/10.1016/j.polymertesting.2020.106595>.
39. Polymer Science: A Comprehensive Reference. Volume 2. Schick C. Elsevier B.V., Amsterdam. 2012; <https://doi.org/10.1016/B978-0-444-53349-4.00056-X>
40. Peterson JD, Vyazovkin S, Wight CA. Stabilizing effect of oxygen on thermal degradation of poly (methyl methacrylate). *Macromol Rapid Commun.* 1999;20(9):480–3. [https://doi.org/10.1002/\(SICI\)1521-3927\(19990901\)20:9%3c480::AID-MARC480%3e3.0.CO;2-7](https://doi.org/10.1002/(SICI)1521-3927(19990901)20:9%3c480::AID-MARC480%3e3.0.CO;2-7).
41. Laachachi A, Cochez M, Ferriol M, Leroy E, Cuesta JL, Oget N. Influence of Sb₂O₃ particles as filler on the thermal stability and flammability properties of poly (methyl methacrylate)(PMMA). *Polym Degrad Stab.* 2004;85(1):641–6. <https://doi.org/10.1016/j.polymdegradstab.2004.03.003>.
42. Chang TC, Yu PY, Hong YS, Wu TR, Chiu YS. Effect of phenolic phosphite antioxidant on the thermo-oxidative degradation of PMMA. *Polym Degrad Stab.* 2002;77(1):29–34. [https://doi.org/10.1016/S0141-3910\(02\)00076-9](https://doi.org/10.1016/S0141-3910(02)00076-9).
43. Lee YM, Viswanath DS. Degradation of poly (methyl methacrylate)(PMMA) with aluminum nitride and alumina. *Polym Eng Sci.* 2000;40(11):2332–41. <https://doi.org/10.1002/pen.11366>.

Publisher's Note Springer Nature remains neutral with regard to jurisdictional claims in published maps and institutional affiliations.

Authors and Affiliations

Alain Alonso¹  · David Lázaro¹ · Mariano Lázaro¹ · Daniel Alvear²

✉ Alain Alonso
alonsoia@unican.es

² General Directorate of Industry, Energy and Mines,
Government of Cantabria, Santander, Spain

¹ GIDAI, Universidad de Cantabria, Avda. Los Castros, s/n,
39005 Santander, Spain